MNRAS **429,** 1342–1353 (2013) doi:10.1093/mnras/sts421

Thomson scattering and collisional ionization in the X-ray grating spectra of the recurrent nova U Scorpii

M. Orio,[1,2]★ E. Behar,[3] J. Gallagher,[2] A. Bianchini,[4] E. Chiosi,[1] G. J. M. Luna,[5] T. Nelson,[6] T. Rauch,[7] B. E. Schaefer[8] and B. Tofflemire[2]

[1]*INAF – Osservatorio di Padova, vicolo dell' Osservatorio 5, I-35122 Padova, Italy*
[2]*Department of Astronomy, University of Wisconsin, 475 N. Charter Str., Madison, WI 53704, USA*
[3]*Department of Physics, Technion, Haifa 32000, Israel*
[4]*Astronomy Department, Padova University, vicolo dell' Osservatorio 3, I-35122 Padova, Italy*
[5]*Instituto de Astronomía y Fisica del Espacio (IAFE/Conicet), CC67, Suc. 28 C1428ZAA CABA, Argentina*
[6]*School of Physics and Astronomy, University of Minnesota, 116 Church St SE, Minneapolis, MN 55455, USA*
[7]*Institute for Astronomy & Astrophysics, Kepler Center for Astro & Particle Physics, Eberhard Karls University, Sand 1, D-72076 Tübingen, Germany*
[8] *Physics and Astronomy, Louisiana State University, Baton Rouge, LA 70803, USA*

Accepted 2012 November 14. Received 2012 November 14; in original form 2012 July 9

ABSTRACT

We present a *Chandra* observation of the recurrent nova U Scorpii, done with the High Resolution camera-S (HRC-S) detector and the Low Energy Transmission Grating (LETG) on day 18 after the observed visual maximum of 2010, and compare it with *XMM–Newton* observations obtained on days 23 and 35 after maximum. The total absorbed flux was in the range 2.2–2.6 $\times$ 10^{-11} erg cm^{-2} s^{-1}, corresponding to unabsorbed luminosity 7–8.5 $\times$ 10^{36} $\times$(d/12 kpc)^2 for N(H) = 2–2.7 $\times$ 10^{21} cm^{-2}. On day 18, 70 per cent of the soft X-tray flux was in a continuum typical of a very hot white dwarf (WD) atmosphere, which accounted for about 80 per cent of the flux on days 23 and 35. In addition, all spectra display very broad emission lines, due to higher ionization stages at later times. With *Chandra* we observed apparent P Cygni profiles. We find that these peculiar profiles are not due to blueshifted absorption and redshifted emission in photoionized ejecta, like the optical P Cyg of novae, but they are rather a superposition of WD atmospheric absorption features reflected by the already discovered Thomson scattering corona, and emission lines due to collisional ionization in condensations in the ejecta. On days 23 and 35, the absorption components were no longer measurable, having lost the initial large blueshift that displaced them from the core of the broad emission lines. We interpret this as an indication that mass-loss ceased between day 18 and day 23. On day 35, the emission line spectrum became very complex, with several different components. Model atmospheres indicate that the WD atmospheric temperature was about 730 000 K on day 18 and reached 900 000–1000 000 K on day 35. This peak temperature is consistent with a WD mass of at least 1.3 M$_\odot$.

Key words: stars: individual: U Scorpii – novae, cataclysmic variables – white dwarfs – stars: winds, outflows – X-rays: binaries – X-rays: individual: U Scorpii.

1 INTRODUCTION

The recurrent nova (RN) U Scorpii is one of a handful of such objects known in the Galaxy, although this class may be much more numerous than we have been able to assess so far. 'Recurrent' means that the thermonuclear flash is repeated on a human time-scale. The outburst supposedly recurs also in classical novae; however, the time-scales can be as long as several times 10^5 yr on white dwarf (WD) at the low end of the nova mass distribution (0.6–0.7 M$_\odot$), accreting matter at a low rate of $\leq 10^{-11}$ M$_\odot$ yr^{-1} (see Yaron et al. 2005, and references therein). The models predict that RN occurs either with moderately high accretion rate $\dot{m}$ on WD of about 1 M$_\odot$ or at very high $\dot{m}$ ($M \geq 10^{-8}$ M$_\odot$ yr^{-1}) on WD with $M \geq$ 1.2 M$_\odot$. The velocity of the ejecta increases, and the duration of the outburst decreases, with the WD mass. About half of all RNe are *symbiotic novae*, that is systems with a giant secondary and a hot WD, with orbital periods of hundred of days (as opposed to most classical novae, which have orbital periods of hours and main-sequence companions).

★ E-mail: marina.orio@oapd.inaf.it

U Sco has an orbital period of 1.23 d and belongs to the class of RNe with a near-main-sequence or moderately evolved secondary (Schaefer 1990; Schaefer & Ringwald 1995). The secondary spectrum is not detected in optical spectra at quiescence, but at a late post-outburst phase Anupama & Dewangan (2000) measured the spectral features of a K2 subgiant. In the previous outbursts the ejecta were extremely depleted in hydrogen (Barlow et al. 1981), so the secondary must have lost a significant fraction of its hydrogen-rich envelope. At quiescence, He II lines are dominant in optical spectra and the hydrogen lines are absent or weak, a fact that has been interpreted as accretion of He-rich material from a H-depleted secondary (e.g. Duerbeck et al. 1993). Although Maxwell et al. (2012) cast doubts on the high He abundance, the possibility of very enhanced helium in U Sco is very interesting as it may result in a Type Ia supernova (SN Ia) without a hydrogen-rich envelope, which is consistent with the upper limits on hydrogen in the SN Ia spectra.

The short and luminous outburst of U Sco was observed 10 times (1863, 1906, 1917, 1936, 1945, 1969, 1979, 1987, 1999, 2010), with peak magnitude $V \simeq 7.5$, decay times by 2 and 3 optical magnitudes, $t_2 = 1.2$ and $t_3 = 2.6$ d, respectively, and a return to quiescence within 67–68 d. These parameters indicate a very massive WD, such that sufficient pressure for a thermonuclear runaway is built up at the base of the envelope even with a small accreted envelope (e.g. few $\leq 10^{-7}$ $M_\odot$; see Starrfield, Sparks & Shaviv 1988). We adopt 12 ± 2 kpc as distance to the nova, measured thanks to its eclipse in the optical (Schaefer et al. 2010).

Since U Sco has shown outbursts on an almost regular time-scale of 10 ± 2 yr (assuming that a couple of eruptions were missed because they occurred when the nova was behind the sun), Schaefer (2011) was able to predict the last eruption of 2010 January with an uncertainty of only 1 yr. When the event occurred, a strategy was in place to observe the outburst at all wavelengths.

In this paper we present grating X-ray spectra, the only means to probe the effective gravity, chemical composition and effective temperature of the underlying WD once the photosphere shrinks back to the WD radius (e.g. Nelson et al. 2008, and references therein). One observation was proposed by us, 17 d after the visual maximum with the *Chandra* LETG grating. We adopt here the epoch of the observed visual maximum 2010-01-28.1 (JD 245 522 5605) as the initial time (although Schaefer 2011 extrapolated the light curve concluding that the peak had occurred a few hours earlier). Two *XMM–Newton* observations were done on 2010-02-19 at 15:41:09 UT, and on 2010-03-14 at 14:33:32 UR, 22 and 35 d after maximum, respectively (note that for the different *XMM–Newton* detectors the beginning of the observations varies slightly, and for details see also Ness et al. 2011a, 2012; Orio 2011).

In addition to presenting and analysing the early *Chandra* spectrum, in this paper we compare it with the *XMM–Newton* Reflection Grating Spectrometer (RGS) grating spectra. The proposers of one of these observations, Ness et al. (2012), have analysed the X-rays and UV data and examined the time variability in these two bands in detail. They found that a partial eclipse of the X-ray continuum can be explained only if the hot central source is observed after having been Thomson scattered, a conclusion that we reached independently (Orio 2011), and with which we fully agree. These authors remark about the lack of absorption lines, expected and usually observed in novae in outburst in X-rays, and attribute it to possible 'smearing' by Thomson scattering. They also describe and examine the spectra, proposing lines' identifications and attributing the emission lines to resonant scattering. In this work, we found that the nova development with time, including the *XMM–Newton* observations, is fundamental to fully understand the physics of the X-ray grating spectra. Without the intent to replicate the Ness et al. (2012) work, we analyse and attempt to model with detailed physics all the grating X-ray spectra, thereby reaching different conclusions than the above authors on the origin of the emission lines observed with *XMM–Newton* and on the reason for the lack of absorption features at late stages.

In Section 2 we describe the observations, the data extraction method, and when the observations occurred in the context of the long-term X-ray evolution. In Section 3 we show the short-term light curve, which we find relevant to understand the physics of the spectra. In Section 4 we discuss the apparent P Cyg profiles observed in the *Chandra* spectrum. After having analysed the origin and meaning of these features, we performed atmospheric fitting for all spectra, and evaluated temperature evolution and peak temperature (Section 4). In Section 5 we discuss the physical mechanisms producing the emission lines and how we attempted a global fit; finally, conclusions are presented in Section 6.

2 THE OBSERVATIONS AND THEIR POSITION IN THE LONG-TERM LIGHT CURVE

The *Swift* satellite monitored U Sco almost daily on all dates when it was technically possible. We extracted the *Swift* data and present the X-Ray Telescope (XRT) X-ray light curve in Fig. 1. Although this paper's focus is on the longer observations done with *Chandra* and the comparison with the RGS of *XMM–Newton* data, the *Swift*-XRT long-term light curve puts the data in the context of the outburst evolution. The arrows indicate the times at which the grating observations were done. The X-ray flux was still on the rise during both the 2010-02 observations (days 18 and 23), while the maximum X-ray flux was recorded around the date of the third and final X-ray grating observation in March, on day 35. The X-ray spectrum remained remarkably soft during the whole post-outburst phase, with more than 95 per cent of the counts below 0.7 keV. A sharp decay followed the March observation until day 67, when the

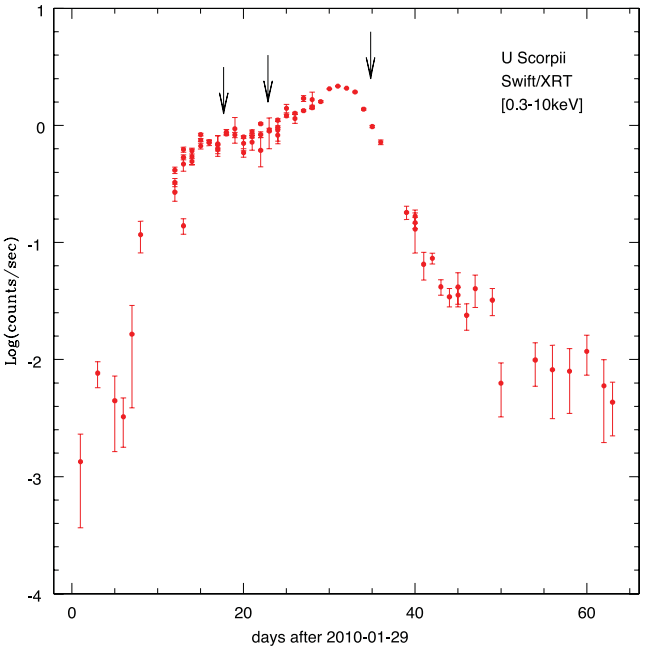

Figure 1. *Swift*-XRT count rate versus time measured since the recorded outburst on 2010-01-29, in the 0.2–10 keV range.

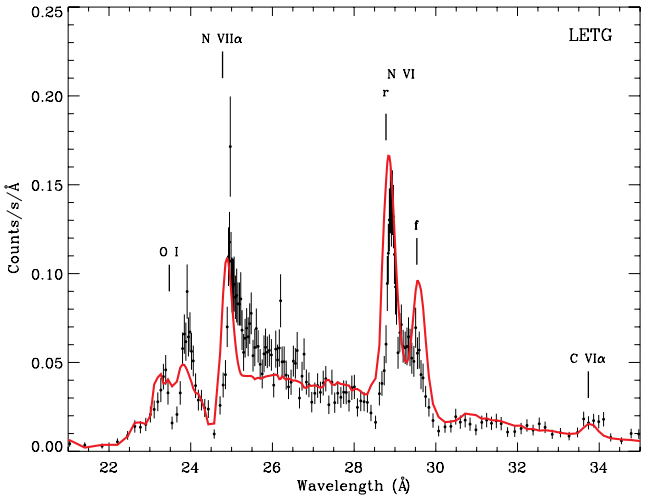

Figure 2. The U Sco spectrum measured with the *Chandra* LETG grating on 2010-02-14, day 18 post-optical maximum in the *V* band (+1 and −1 orders have been summed). The red solid line shows the best fit with two components: an atmospheric model with a 740 000 K $T_{\rm eff}$ and a collisionally ionized optically thin plasma with tenfold He and N abundances with respect to solar, and plasma temperature $kT = 93$ eV (see Table 2).

nova was almost back to X-ray minimum. Further information on the UV and X-ray evolution observed with *Swift* can be found in Ness et al. (2012).

The first grating observation of U Sco was proposed by us and was done with the LETG/HRC-S instrument of the *Chandra* observatory on 2010-02-14, at 11:38:22 UT. As stated above, this was day 18 after optical maximum in the *V* band (see Schaefer et al. 2010). The exposures lasted for 23 ks (6.38 h). The observed count rate spectrum is shown in Fig. 2, while Fig. 3 shows the fluxed spectrum, compared with the spectra measured with the *XMM–Newton* RGS gratings on days 23 and 35. Fig. 2 also shows a model fit, discussed in detail in Sections 4 and 5. In order to extract the LETG spectrum, we applied the most updated calibration to the LETG pipeline-processed level 2 *event* and *pha Chandra* data files. Response matrices and ancillary response (effective area) files were created using the tools mkgrmf and mkgarf, part of the CIAO v4.2

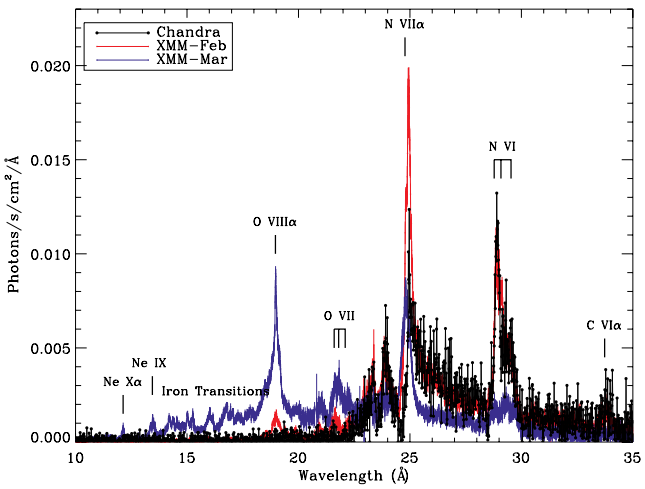

Figure 3. Measured flux versus wavelength in the three grating spectra on days 18, 23 and 35 after the discovery, The *Chandra* spectrum is displayed in black, the averaged RGS1–RGS2 spectrum of 2010-02-14 is plotted in red and the 2010-03-02 RGS1–RGS2 spectrum is in blue.

package. We measured a summed ±1 order count rate of 0.477 ± 0.008 counts s^{-1} in the 0.2–0.8 keV energy range in which flux is measurable above the background (corresponding to approximately 15–60 Å in wavelength range). We measured an unabsorbed flux of 2.2 ± 0.2 erg cm^{-2} s^{-1}. In Fig. 3, the strongest lines of the three spectra are labelled (for additional lines' identification, see Table 1).

We see in Fig. 2 that for at least three lines (the Ne VI Heγ line with rest wavelength 23.77 Å, the N VII hydrogen α line with rest wavelength 24.78 Åand the resonance line of the N VI triplet at 28.78 Å) the emission portion appears redshifted and the absorption wing blueshifted. This is intriguingly similar to the P Cyg profiles observed in optical spectra.

We compared the *Chandra* spectrum with archival *XMM–Newton* grating spectra obtained on 2010-02-19 at 15:41:09 UT and on 2010-03-3 at 14:33:32 UT, (5 and 17 d later, respectively, days 23 and 35). The *XMM–Newton spectra* were extracted with XMM-SAS version 11.0.2. There was variability during both *XMM–Newton* observations, as we discuss in the next section, but in February (day 23 after the outburst) we measured average count rates of 0.881 ± 0.004 and 0.824 ± 0.004 counts s^{-1} with the RGS1 and RGS2 gratings, respectively, while in March (day 35) the average count rates were 1.037 ± 0.005 and 0.951 ± 0.004 counts s^{-1}. The unabsorbed flux seems was rising moderately, and we measured 2.5 ± 0.2 × 10^{-11} and 2.6 ± 0.2 × 10^{-11} in the second and third observations, respectively. All *XMM–Newton* instruments were observing the nova simultaneously, including the Optical Monitor, and the broad-band X-ray imagers EPIC-pn and MOS1 and MOS2. The RGS spectra are shown in Figs 3–5. Figs 4 and 5 present the count rate spectrum (like Fig. 2 for *Chandra*). The fit with atmospheric and plasma emission models, also shown in the figures, is discussed in detail in Sections 4 and 5.

3 THE SHORT-TERM LIGHT CURVE: A SIMULTANEOUS X-RAY AND OPTICAL ECLIPSE

At optical wavelengths, the eclipse of the accretion disc by the K dwarf companion was discovered and measured at quiescence by Schaefer & Ringwald (1995), and it was observed again in the outburst by Schaefer et al. (2011), indicating that the accretion disc had already been reestablished by the third week after the optical maximum. The orbital period of U Sco is 1.230 546 95 d (Schaefer & Ringwald 1995). For the ephemeris we assume in this paper the result of the linear fit for the whole 1999–2010 intereruption interval, with an HJD time of the optical minima 245 1234.5387 + N×1.230 546 95. We caution that the many observed eclipses during the last four eruptions show significant deviations of the minimum from this ephemeris, with the offsets changing throughout the eclipse. This means that the centre of optical light curve changes throughout the eruptions and is not exactly at the same position during the quiescent periods.

We did not detect significant variability in the *Chandra* zero-order light curve, but all the observation occurred outside the eclipse observed in optical. The exposure started at orbital phase 0.4463 and covered almost a quarter (22 per cent) of the period.

Both *XMM–Newton* observations covered about 60 per cent of the orbital period and thus overlapped with the optical eclipse time. The day 23 observation started at phase 0.84, and the one of day 35 started at phase 0.55.

In Fig. 6 we present the *XMM–Newton* EPIC-pn light curves and compare them with the optical light curves of Schaefer et al.

Table 1. Rest, measured wavelength and fluxes in photons cm^{-2} ks^{-1} for the emission lines identified and measured in the three grating spectra. See the text for an evaluation of the errors in the flux estimate.

Line	λ_0 (Å)	*Chandra* 02-14 λ_m (Å)	Flux	*XMM* 02-19 λ_m (Å)	Flux	*XMM* 03-05 λ_m (Å)	Flux
C VI Lyα	33.7342	33.78 ± 0.02	0.39	33.78 ± 0.05	0.43	33.75 ± 0.05	
N VI f	29.5346	29.50 ± 0.02	0.93	29.50 ± 0.03	1.23	29.60 ± 0.05	0.35
N VI i	29.0819	29.16 ± 0.02	0.91	29.20 ± 0.02	1.65	29.22 ± 0.05	0.42
N VI r	28.7800	28.93 ± 0.02	2.20	28.82 ± 0.05	2.10	28.80 ± 0.05	0.31
C VI Lyγ	26.990	26.80 ± 0.02					
N VI Heβ	24.90				≤3.8	24.95 ± 0.01	≤1.3
N VII Lyα	24.78	24.94 ± 0.03	1.71	24.92 ± 0.03	5.64	24.80 ± 0.02	2.51
N VI Heγ	23.771	23.81 ± 0.05	0.43	23.81 ± 0.05	0.60	23.82 ± 0.02	2.70
O VII f	22.097			22.108 ± 0.050		22.13 ± 0.05	0.30
O VII i	21.801			21.807 ± 0.020	≤0.24	21.80 ± 0.02	0.49
O VII r	21.602			21.603 ± 0.050	0.35	21.61 ± 0.02	0.39
O VIII Lyα	18.969			19.05 ± 0.03	0.74	19.00 ± 0.02	3.21
O VII Heβ	18.627			18.57 ± 0.05		18.55 ± 0.02	
Fe XVII	16.78			16.78 ± 0.05		16.80 ± 0.05	
O VII Lyβ	16.00			15.95 ± 0.03		16.00 ± 0.02	0.44
Fe XVII	15.262			15.30 ± 0.05		15.25 ± 0.05	≥0.10
Fe XVII	15.01			15.15 ± 0.02		15.03 ± 0.05	0.12
Fe XVIII	14.207					14.22 ± 0.03	0.13
Fe XIX	14.667			14.70 ± 0.05		14.67 ± 0.03	
Ne IX f	13.6984						
Ne IX i	13.5503					13.57 ± 0.05	0.12
Ne IX r	13.4474			13.45 ± 0.02		13.48 ± 0.05	0.15
Ne X α	12.1321					12.14 ± 0.05	0.15
Ne IX Heβr	11.55					11.60 ± 0.10	
Mg XI He r	9.09			9.20 ± 0.03		9.20 ± 0.03	

(2010) measured in the same two weeks during which the two X-ray data sets were taken. All light curves are folded over the optically measured orbital phase and repeated twice. For the X-ray light curve, we plotted a quantity that is 2.5 times the logarithm of the X-ray flux normalized to its minimum value, for a direct comparison with optical magnitudes. The EPIC-pn exposures are 63 185 and 62 318 s long, respectively.

On day 23 in the X-ray light curve the most evident oscillation is a pronounced one with a semi-regular (albeit not regular) period of about 3 h, extensively discussed by Ness et al. (2012). These authors also extracted the spectrum in and out of the oscillation, showing no variation of the emission lines. The authors attribute the phenomenon to large clumps, of absorbing material at a distance of about 3.5 $R_\odot$ from the WD, intersecting the line of sight in the direction of the accretion stream, during the process of re-establishment of the disc. We do not wish to further discuss these oscillations, although we suggest that this semi-regular period (even if it is associated with ejection of parcels of material) may represent the disc rotation period, which may be slightly variable while the disc is still being formed.

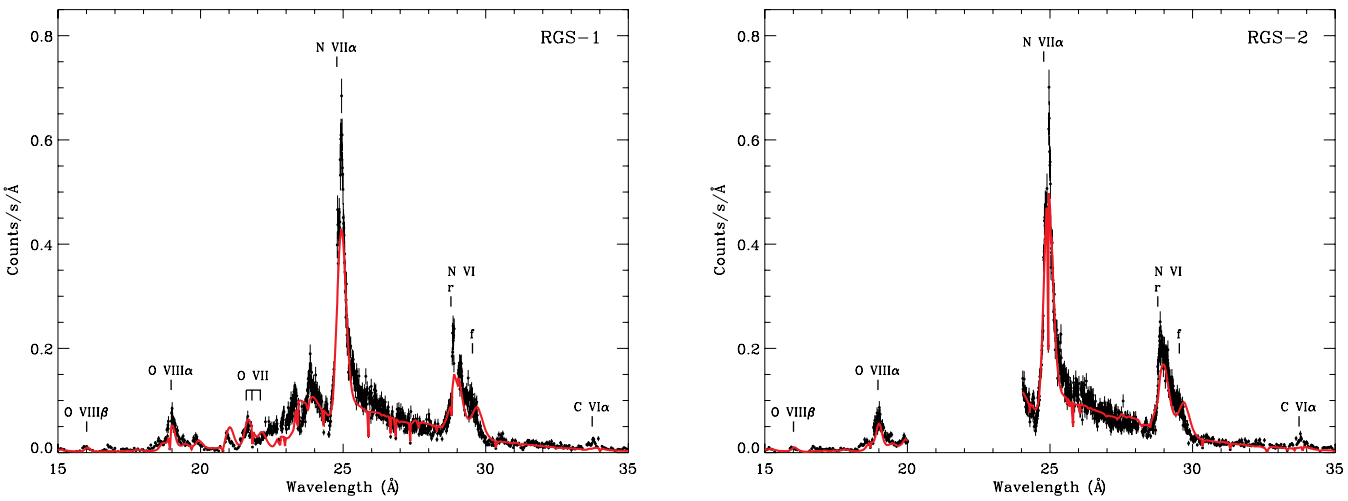

Figure 4. The *XMM–Newton* RGS-1 (left) and RGS-2 (right) spectra of U Sco on day 23 after the optical maximum. The red line shows the fit with a WD atmosphere with absorption lines blueshifted by 2000 km s^{-1}, with both BVAPEC components as in Table 2 or adding the second BVAPEC component for the RGS-2 hard portion of the spectrum.

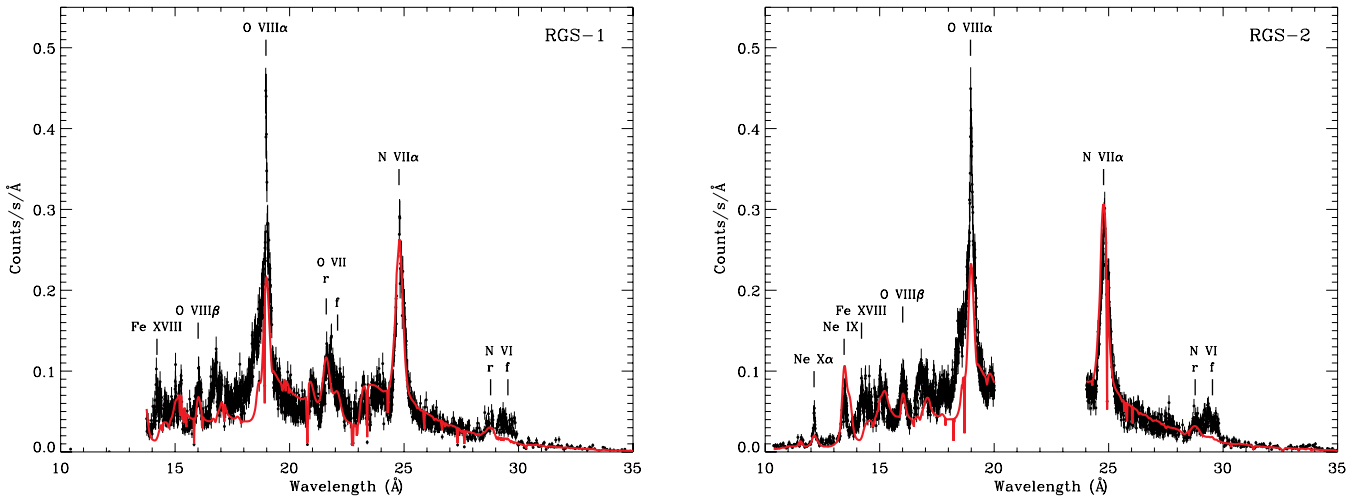

Figure 5. The *XMM–Newton* RGS-1 (left) and RGS-2 (right) spectra of U Sco on day 35 after the optical maximum. The fit is shown in red, the parameters are given in Table 2.

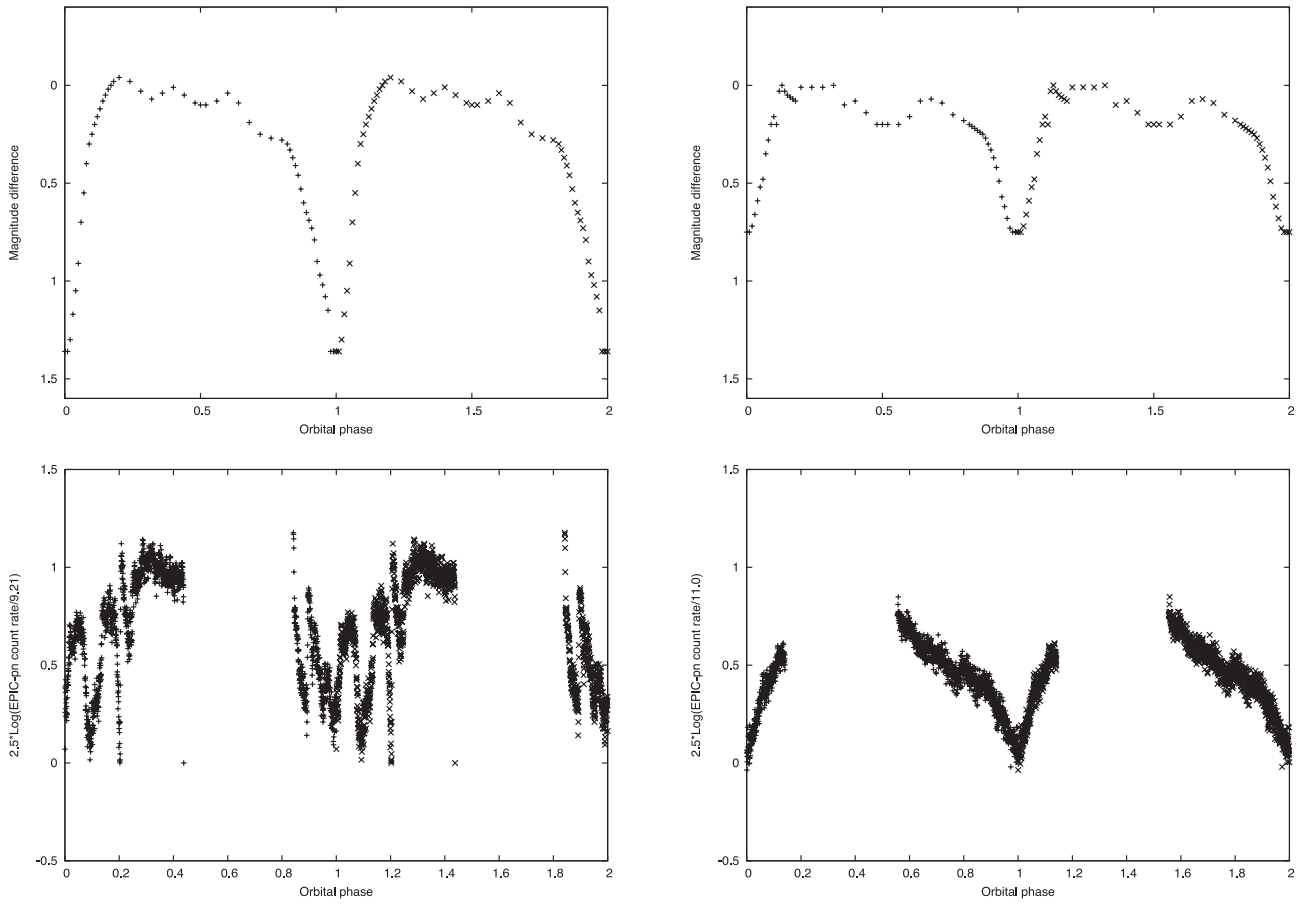

Figure 6. The average optical *V* magnitude light curve of U Sco during days 21–26 (left-top panel) and days 32–41 after visual maximum (right-top panel; Schaefer et al. 2011), compared with the observed X-ray light curve measured with the EPIC-pn instrument aboard *XMM–Newton* on day 23 (left-bottom panel) and on day 35 (right-bottom panel). The logarithm of the count rate normalized to the minimum value of the measurements and multiplied by 2.5 is plotted as a function of phase, to match the magnitude scale. The light curve was binned in time with 50 s bins before conversion to phase, on days 23 (right) and 35 (left) after the outburst.

A clear orbital modulation in the day 35 spectrum was noted by us and by Ness et al. (2012). These authors also stress that almost all emission lines observed in the spectra are not eclipsed, while the continuum is, and we agree with their analysis. However, we cast some doubts regarding the dimming in eclipse of only one specific line, the O VIII Lyα (the above authors remark that this is the only line that seems to vary, even there is clearly no variation of the O VII triplet). Extracting the spectrum over the short duration

of the eclipse we find a variation of this line only at the 2σ level, so we suggest that this is not statistically significant. In any case, the main purpose of Fig. 6 is to show that the orbital modulation seems already clearly present in the *XMM–Newton* EPIC-pn light curve of day 23, although it is not as pronounced as on day 35. On day 35, the average count rate during orbital phases 0 to 0.12 and 0.88 to 1 is 0.75 and 0.84 counts s^{-1} with RGS1 and RGS2, respectively, while we measured 1.10 and 1.05 counts s^{-1} with RGS1 and RGS2, respectively, during the rest of the observation. We find that the variation in count rate in and out of eclipse, outside the $\simeq$3 h oscillations, is by at least 25 per cent even on day 23.

Because the eclipse takes out only about 50 per cent of the flux in the X-ray continuum, on day 35 a large portion of this continuum must originate in a much more extended region. We assume that this is a Thomson scattering corona, reprocesses a fraction of the WD radiation in an achromatic way (Ness et al. 2011a, 2012; Orio 2011). The inclination angle in U Sco is $82\overset{\circ}{.}7 \pm 2\overset{\circ}{.}9$ (Thoroughgood et al. 2001), so it is quite conceivable that we did not observe most of the WD flux directly. The accretion disc was placed by Schaefer et al. (2011) at 3.4 $R_\odot$ distance from the WD in a light-curve model for day 35. Because of the nearly edge-on inclination, the short-duration and deep X-ray eclipse does not appear to be due to the disc. We assume that the source of the continuum is eclipsed by the secondary, exactly like for the eclipse of the disc by the secondary observed at quiescence at optical wavelength. Following the reasoning of Schaefer et al. (2011, see their fig. 13 for the optical eclipse) we conclude that most of the continuum is observed as reflected at a distance equal to or larger than the 3.4 $R_\odot$ distance from the WD at which Schaefer et al. place the outer rim of the disc.

We intend to show that the *Chandra* spectrum with its absorption features is best explained assuming that this scattering corona was already present, and at comparable distance from the WD, on day 18, although no X-ray observations at eclipse minimum were done.

4 FITTING THE SPECTRUM, STEP BY STEP: THE WD

4.1 The absorption lines observed with *Chandra*

Two puzzles are immediately apparent when we examine Figs 2–5. First of all, the *Chandra* spectrum shows deep absorption features of nitrogen, while the *XMM–Newton* ones do not display any features in absorption. Although model atmospheres show that the absorption becomes less pronounced at high temperatures (Rauch et al. 2010), the models predict deep absorption features of nitrogen, always detected in the previous X-ray gratings' observations of other novae (e.g. Rauch et al. 2010, Ness et al. 2011b). The other surprising element, as we already noted, is the apparent P Cyg-like profiles in the *Chandra* spectrum. P Cyg profiles are typical of the optical spectrum of novae in X-rays, but they have never been observed in their X-ray grating spectra, except (possibly) in the first *XMM–Newton* spectrum of another fast RN, LMC 2009 (Orio 2012).

Emission lines attributed to the ejecta were observed in the X-ray spectra of several other novae (Drake et al. 2003; Ness et al. 2003; Nelson et al. 2008; Rauch et al. 2010). Are the absorption wings of these 'P Cyg profiles' in this U Sco spectrum produced in the nova shell, instead of being due to the WD? At least one profile cannot be a P Cyg in the conventional sense, and it is the one of the N VI Heγ line. The absorption in this case is not of the same line, but it is mainly of another overlapping line at zero velocity, due to the O I 1s–2p transition at $\sim$23.476 Å, which does occur in the interstellar medium along the line of sight to U Sco. The fact that this absorption feature was hardly measurable in N LMC 2009, in one LETG spectrum that appears similar to this one (Orio 2011, 2012), confirms the identification because N LMC 2009 is in a direction of much lower interstellar absorption [N(H) $\simeq 4 \times 10^{20}$ cm^{-2}]. Thus, we realize that at least this particular P Cyg-like profile is in fact only a sort of 'pseudo-P Cyg', composed of an absorption and an emission feature that do not have origin in the same medium.

We examine now the P Cyg profiles of the other two strong lines, shown in Fig. 7, to understand whether they may be due to the 'real', classic P Cyg phenomenon. As Fig. 7 shows in velocity space, the N VII emission appears blueshifted by 2200 $\pm$ 200 km s^{-1} in absorption, and redshifted by the same amount in emission. The N VI resonance line with rest wavelength 28.78 Å is instead blueshifted by 2700 $\pm$ 300 km s^{-1}, in absorption, and redshifted by 1500 $\pm$ 300 km s^{-1} in emission, so the two components do not cross around zero, but rather towards the red. In the optical spectra of novae, crossing in the red is observed in spectra taken shortly before the P Cyg profile disappears. Typically, the P Cyg profile is no longer observed in the following weeks because the blueshifted absorption becomes negligible compared to the emission. Fig. 8 shows the

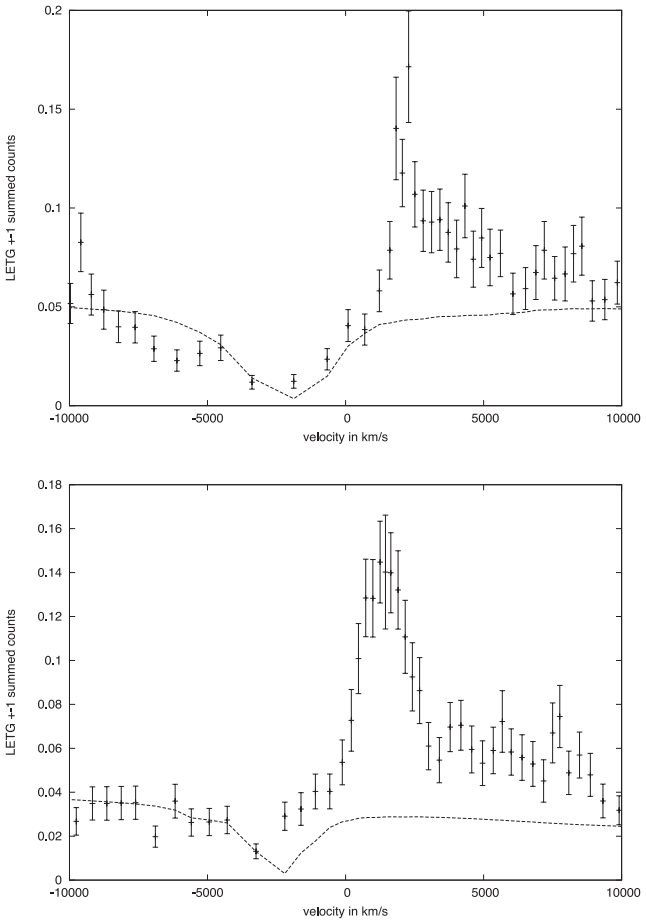

Figure 7. The P Cyg profiles of the Ne VII Hα line (above), and N VI resonance line (below), in the *Chandra* LETG spectrum ($\pm$1 orders summed) plotted in velocity space. The fit with an atmospheric model (see Table 2) with absorption features blueshifted by 2000 km s^{-1} is shown by the dotted line. The two weaker lines of the triplet appear on the right of the resonance line of N VI in emission. There is a contribution of the N VI Heβ line in emission at 24.889 Å (see Table 1).

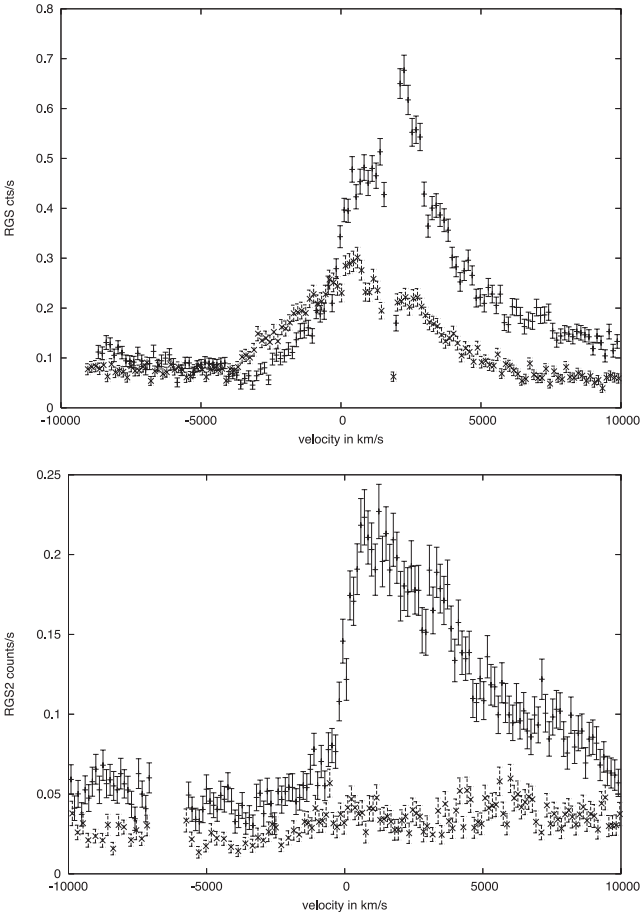

Figure 8. The N VII Lyman α line (above) and N VI resonance line (below) measured with the RGS2 grating in February (dots) and March (crosses), respectively, plotted in the velocity space.

same line profile in velocity space in the RGS spectra of days 23 and 35.

P Cyg profiles in X-ray spectra in general are rarely observed, and the absorption wing, if measurable, is very shallow. This is because in X-rays we are likely to observe outflows and nebulae around compact objects, while in optical we observe them around stars with at least hundreds of times larger radii. This includes the *optical* (as opposed to X-rays) spectra of classical and RNe, where P Cyg profiles at optical wavelengths are observed when the photosphere around the WD has not receded to WD dimensions yet, but is still of the order of at least a solar radius. However, this typically occurs weeks or months before the supersoft X-ray phase, and we expect it only in the first few days, or even in the first hours, in a very fast nova like U Sco. P Cyg profiles at optical wavelengths are due mainly to resonance transitions. The blueshifted absorption is observable only where the material moves in our direction, that is along the line of sight of the photoionizing central object. The optical P Cyg absorption features occur, like the emission, in the 'wind' or nebula around a photoionizing central object, but they are observed in a cylinder with the radius of the central object, and only as long as the radius of the cylinder is not negligible compared to the rest of the shell, from which we observe the emission lines.

Luminous supersoft X-ray continuum – observed in the *Chandra* spectrum as well as in the *XMM–Newton* ones – in novae arises when the central object has shrunk and regained compact dimensions, with a radius of the order of at most 10^9 cm, or else the X-ray luminosity would be largely super-Eddington. Shortly after the outburst, velocities up to 5000 km s^{-1} were measured by Yamanaka et al. (2010), and on day 35 (the day of the last *XMM–Newton* observation), Mason et al. (2012) estimated an expansion velocity of 4000 km s^{-1} from the full width at half-maximum of the optical lines. Assuming this value for the expansion velocity, the nebular ejecta around U Sco at the time of the *Chandra* observation (day 18) had reached a distance from the WD representing almost 300 000 times the WD radius of a very massive WD (1.3 $M_\odot$). The region in which emission occurred was overwhelmingly large in comparison with the cylinder around the line of sight towards the WD. We conclude that the absorption features observed with *Chandra* cannot have been produced in the ejecta. By day 18, any absorption features of the ejecta would already be hidden and embedded in the broad emission lines. There is no evidence of nebular X-ray absorption lines in the ejecta, but in other novae absorption lines were always observed, and they are usually attributed to the WD atmosphere. There is only a recent case in which the blueshifted lines were attributed instead to collisional ionization in a thin outer shell, that of V2491 Cyg (Pinto et al. 2012), but the absorption lines of U Sco are so broad compared to this model, that we can rule out this origin.

We concluded that the velocity of the absorption features also for U Sco was due to a different phenomenon, one causing an intrinsic velocity that had an almost abrupt end, so that the features were still significantly blueshifted on day 18, but not any more a few days later. This process must be mass-loss from the nova. Absorption lines in the X-ray grating spectra of other novae in the early phases were significantly blueshifted, with comparable blueshift to the apparent 'absorption wing' of the 'P Cyg' in the *Chandra* spectrum of U Sco (e.g. Ness et al. 2003; Rauch et al. 2010, for V4743 Sgr; Ness et al. 2011b, for V2491 Cyg). In RS Oph many of the same absorption lines as in the former two novae were observed without measurable blueshift (Nelson et al. 2008). Since the emission lines were strong in a very different range, there was no overlap with WD lines and no apparent P Cyg profile. We conclude that the P Cyg profiles in the *Chandra* spectrum were not 'real P Cyg', but they were rather due to superimposed absorption and emission arising in different regions and different mechanisms. The absorption features were produced in the outmost layer of the WD atmosphere, which was still losing mass, and reflected at a distance of a few solar radii by the *Thomson scattering corona* of the WD. The corona's 'reflection' allowed the lines to be detectable, despite the high inclination angle of the WD in U Sco. Since this corona must have already been present on day 23, we assume that it existed already on day 18 (even if we could not measure a light curve to prove it).

An intrinsic blueshift that lasted while the WD was still losing material in a wind explains why the features were still observable on day 18, even if the emission features are so broadened in U Sco that they should hide the atmospheric absorption. Once the wind from the WD ceased, the absorption line velocity became close to zero, so they were embedded in the centre of the emission lines and were not measurable any longer.

Whatever absorption features may have actually been produced in the ejecta by photoionization, if there was such a phenomenon, were embedded in the emission features long before day 18, due to the small dimensions of the absorption region compared to the fast ejecta. It is also conceivable that the Thomson scattering corona changed in geometry and the WD absorption lines may have become more smeared out between days 18 and 23, and perhaps better 'hidden'. In any case, the transition giving rise to absorption lines

in the atmosphere, even when not observable and measurable, must have occurred until the WD turned off.

4.2 Atmospheric models: the hottest WD

Because of the conclusions above, in order to fit the *Chandra* spectrum, we assumed that the observed absorption components were not produced by photoionization of the ejecta like in the optical P Cyg profiles of novae, but that they originated *inside* the WD atmosphere and were reflected at large distance (>3 R$_\odot$) by the Thomson scattering. We fitted only the continuum of the *XMM–Newton* spectrum. We assume that on days 23 and 25 the atmospheric absorption lines were simply unobservable, hidden by the unusually broad emission lines of this nova once the mass outflow, and with it the blueshift, ceased. Of course, in the *Chandra* spectrum the observed absorption may have been more pronounced if it was not superimposed on emission, so we can only obtain lower limits on the abundances and effective gravity.

Although the *Chandra* spectrum absorption features were eroded by the blue wing of the partially overlapping emission lines, we note that they were still remarkably close in depth and broadening to those observed in other novae without X-ray eclipses, such as V4743 Sgr (Rauch et al. 2010) and RS Oph (Nelson et al. 2008). We adopted the atmospheric models developed by coauthor Thomas Rauch, publicly available on the website http://astro.uni-tuebingen.de/ rauch and developed for very hot WDs, e.g. RS Oph (Nelson et al. 2008) and V4743 Sgr (Rauch et al. 2010). We fitted the spectra with XSPEC, v12.6, assuming that the absorption features were blueshifted by 2000 km s^{-1} (as in Rauch et al. 2010). To date, Rauch's models represent the best approximation to the atmosphere of a hydrogen burning WD, although residual outflows that produce blueshifted absorption are not accounted for in these static models. Models including elements with atomic number up to the one of oxygen are available for a grid of values of effective gravity, with a $\log(g)$ grid from 5 to 9 with 1 step increments. The most recent grid of models, including all elements up to magnesium, was calculated for the hottest WDs, with temperatures above 500 000 K and is suitable for the hot continuum of the U Sco spectra. Since a WD with $T_{\rm eff} > 500\,000$ K must be very compact, the luminosities would become largely super-Eddington with $\log(g) < 9$, and are published only for $\log(g) = 9$.

Model 201 in Rauch's web page was developed specifically with similar abundances to the ejecta of U Sco measured using the optical spectra in the previous outbursts: depleted hydrogen ([He] = 0.489) or a helium mass fraction of 70 per cent, and almost 50 times enhanced nitrogen with respect to the solar value ([N] = 1.668). We fitted models of this grid with XSPEC, after blueshifting the absorption features by 2000 km s^{-1}. We do not obtain the best fit with model 201, but rather with model 003, with [He] = 0.382 and [N] = 1.803. This is not surprising, because the abundances in the burning layer can be quite different from those of the ejecta, where mixing with unburned material has occurred.

The final product in our fit, shown in Fig. 2 for the *Chandra* LETG, is a composite model of WD atmosphere and superimposed emission lines, but for the *Chandra* spectrum we started by performing an experiment, ignoring the channels containing the strong emission lines (24.8–25.6 Å for N VII Lyα and 28.7–30.0 Å for the N VI triplet), so that the model fit was better constrained by the continuum and by the absorption features. For the composite fits plotted in blue in Figs 2, 4 and 5 we binned the data with 30 to 50 counts per bin, but for the initial experiment, in order to retain the high spectral resolution of the LETG, we binned the data only by a factor of 4 resulting in wavelength bins of 0.01 Å. With a low resulting number of counts in each bin, we used the C statistic (Cash 1979) rather than the more commonly used χ^2 statistic. We found that the C parameter is smallest for the smallest C/N ratio (typical of CNO ashes) and steadily increases as the C/N ratio increases. The decrease of the 'C' parameter with C/N ratio is about 20 per cent from model 011 to model 003 of Rauch's grid. All models with solar abundances yield poor fits to the *Chandra* LETG spectrum. The temperature for the 'truncated-emission' spectrum in the 2σ confidence range ($\pm 2\sigma$) is 650 000–750 000 K. The best fit yielded a temperature of 730 000 K, N(H) = 2.5 $\times$ 10^{21} cm^{-2} and an absorbed flux of 1.64 $\times$ 10^{-11} erg cm^{-2} s^{-1}, corresponding to an unabsorbed flux of 4.2 $\times$ 10^{-10} erg cm^{-2} s^{-1}. The bolometric luminosity of the WD in this model is 7.2 $\times$ 10^{36} $\times$ (d/12 kpc)^2.

We fitted also the spectra observed later with *XMM–Newton*, although there are no absorption features to better constrain the temperature range. The fit returns almost the same temperature for days 18 and 23. In the spectrum of day 35 the fit yields instead a higher temperature, in the range 900 000–1100 000 K, and is unvaried if we add the emission component, discussed in Section 5. The WD temperature at maximum X-ray luminosity is tightly correlated with WD mass. We know from the models that the effective temperature exceeds 900 000 K only for WD mass of around 1.3 M$_\odot$ (Yaron et al. 2005).

The models yield an absorbed WD luminosity of around 7 $\times$ 10^{36}, which at 12 kpc distance is a factor of 5–10 smaller than the luminosity so far measured in other WDs with even lower peak temperature (e.g. Balman, Krautter & Ögelman 1998; Orio et al. 2003; Nelson et al. 2008). For the other novae, the WD luminosity at peak was several times 10^{37} erg s^{-1}. We explain also this puzzle, like the one posed by the apparent P Cyg profiles, if we assume U Sco we did not observe the WD directly. The reprocessing factor for the WD radiation must have been of the order of 10 per cent.

We note that after the previous outburst in 1999, Kahabka et al. (1999) fitted the *BeppoSAX* low-resolution, low-S/N LECS spectrum with a WD atmospheric model. They derived a luminosity in the range 2.7–18 $\times$ 10^{37} $\times$ (d^2/12 kpc) 19–20 d after the optical maximum, and an effective temperature of 75 eV (870 000 K). The count rate was however only 0.06 counts s^{-1}, a value that appears too low by a factor of about 2 if translated into both the *Chandra* and *XMM–Newton* count rates with PIMMS for a blackbody at 75 eV and N(H) = 2.5 $\times$ 10^{21} cm^{-2}. The *BeppoSAX* observation lasted for about 14 h, so the low count rate is not explained with orbital variability. We cannot reconcile it with the lower luminosity of the present WD component. Probably the atmospheric model had significant differences from the most recent and detailed models of Rauch, but we also cannot rule out that the fit was correct, and the Thomson scattering corona may have been very different, or not present, in the previous outburst.

5 THE ORIGIN OF THE EMISSION LINES: SHOCKS, CONDENSATIONS AND AN EVOLVING VIOLENT MEDIUM

In the *Chandra* spectrum 20 per cent of the flux was in the emission features, and in the RGS spectra about 30 per cent, while the remaining flux was due to the continuum. Despite small uncertainties in the relative calibration of the *Chandra* and *XMM–Newton* instruments, as we see in Fig. 3, the spectra are remarkably similar on days 18 and 23. However, two striking changes happened: the

absorption features seem to have disappeared except for O I at 23.476 Å, which we identified as interstellar in origin, and oxygen emission lines suddenly appeared. The O VIII line, which is not measurable in absorption in the WD atmosphere on day 18 but is clearly detected in emission with *XMM–Newton* on day 23, was almost symmetric around zero velocity since it appeared, consistently with no erosion by a nearby blueshifted absorption line. This does not imply that the line did not exist at all in the WD atmosphere, because the level of the WD continuum in that energy range is too low to measure absorption (see Rauch et al. 2010).

In emission, the full width at half-maximum of this line is approximately 4000 km s^{-1}, which is consistent with the velocity measured in the optical spectra of Mason et al. (2012). As can be seen comparing Fig. 7 with Fig. 8, the emission features in the third spectrum appear symmetrical around the rest wavelength of the line, and have an almost triangular shape, indicating that lines are produced in an optically thin expanding medium. In contrast, the profiles of the emission lines in the optical spectra of novae after the P Cyg profiles have disappeared usually appear flat-topped, indicating that the expanding medium is optically thick.

We measured the emission line fluxes by fitting the strongest lines with Gaussian profiles, and we attempted a fit to a few weak lines with triangles. The photon flux is given for each line in the three spectra in Table 1. We estimate that our measurements are accurate to within 10 per cent for isolated lines and flux above approximately 0.4×10^{-4} photons cm^{-2} ks^{-1} (which were fitted with a Gaussian). The accuracy is probably not more than $\simeq$25 per cent below this value (where we fitted a few lines with a triangle, especially for the day 35 spectrum). We did not attempt to measure line fluxes below 0.12 photons cm^{-2} ks^{-1}, because the uncertainty seems very large below this value, but in some cases we can still identify lines with probably almost an order of magnitude lower flux (e.g. Mg XI in the last spectrum).

The emission lines, much less strong in this wavelength range in other novae, in the U Sco spectra are very pronounced and broad (compared with thermal and instrumental broadening; see e.g. Brinkman et al. 2000; Ness et al. 2003). We attribute the line broadening to the expansion velocity of the nova shell, like the broadening often observed in the optical spectra. The RNe LMC 2009 (Orio 2011) and T Pyx (Tofflemire et al. 2012) have been the only other ones with broad emission features. We also note that the carbon lines are much weaker than those of nitrogen. Only the C VI Lyα line in emission at 33.90 $\pm$ 0.12 Å (rest wavelength 33.7342 Å) is clearly detected.

5.1 A comprehensive spectral fit: days 18 and 23

In Figs 2, 4 and 5 we plotted in red the fit to the lines and continuum obtained with physical models. These models can be regarded as a sort of first-order approximation to the correct model to explore the relevant physical mechanisms in these spectra. We have not reached a perfect fit, as the value of the reduced χ^2 in these fits varies from 2.7 (Fig. 2) to 4 (Fig. 5). Rather than obtaining a statistically significant fit, we focused on good qualitative agreement and on reproducing the emission line ratios as well as possible. We think that as nova observations are continued in the next few years, we should be able to gather many more details of the nova physics, which will allow us to fine-tune these models of the very complex phenomena occurring in nova WD atmospheres and in their ejected shells.

On days 18 and 23, the relative line strength, combined with the lack of a broad radiative recombination Radiative Recombination Continua (RRC) feature of N VI at 22.5 Å, which should be clearly present in the case of photoionization (e.g. X-ray spectra of planetary nebulae or some AGN; see fig. 5 of Kinkhabwala et al. 2002), indicates that the transitions are due to collisional ionization. We used the XSPEC package, v12.6, adding to the atmospheric model of the previous section and a component of collisional ionization, namely the BVAPEC model, that allows us to include velocity broadening (1σ value, which corresponds to the half-width at half-maximum of the lines). Table 2 gives relevant parameters of the spectral fits shown in the figures. We assumed that helium in the plasma component is enhanced 10 times with respect to solar values. In order to improve the fit to the emission lines, we need a large overabundance of nitrogen also in the BVAPEC component, at least 10 times the solar value, and even up to 70 times like in the fit we show in Fig. 2 for the *Chandra* spectrum (this is the best fit with only two components, although we obtained slightly worse, but similar fits with an enhancement by a factor of 10 and a slightly different set of parameters). We note that the WD unabsorbed luminosity resulting from these fits is reduced by up to 30 per cent with respect to the values contained in the 'experiment' in Section 4.1, in which we fitted only the continuum, cutting the prominent emission features.

Figs 2 and 4 show that we can reproduce the relative strength of most lines by assuming collisional ionization lines with the Table 2 models for days 18 and 23. However, the BVAPEC collisional ionization model in XSPEC assumes a low-density limit and does not predict that the forbidden line is quenched compared to the intercombination line. We see in Figs 2 and 4 that the N VI λ29.5446 forbidden line, the N VI triplet on days 18 and 23, and the O VII λ22.097 line on day 23 are less strong than in the models shown in the figures.

We attribute this phenomenon to line formation in a zone of such high density that the collisional de-excitation rates are close to the radiative decay rates. When the two rates are comparable, the radiative decay fraction from an excited level is reduced and so the emission becomes weaker. The electron density n_e at which the N VII forbidden line is de-excited is a few times 10^9 cm^{-3} (Ness et al. 2001; Chen et al. 2004). This density is not unheard of for nova shells in the first few weeks after the outburst. n_e of order of 10^{12} cm^{-3} was derived by Neff, Smith & Katelsen (1978) from the analysis of the optical spectra of V1500 Cyg.

This high density is higher than the value derived from the emission measure in the fit in Table 2, n_e = a few times 10^7 with the assumptions of the model, *if the ejected shell volume is uniformly filled*. Since estimates of the ejecta mass of U Sco converge varying from a few 10^{-6} $M_\odot$ to a few 10^{-7} $M_\odot$ (see Schaefer 2011, Starfield et al. 1988), assuming uniform filling of the shell, we expect that n_e does not exceed a few times 10^5 on day 18, and it should be decreasing as the ejecta expand. This discrepancy implies an emitting volume of the order of only 10^{-4} the volume of the shell. The explanation seems to be that line emission occurs in dense condensations. We note that the large clumps that explain the light curve $\simeq$3 h period in the Ness et al. (2012) model occupy a much smaller fraction of the shell volume corresponding to only a few times 10^{-9}. Clumpiness is not completely unexpected, and it has often been invoked to explain nova optical spectra, starting with the pioneering work of Gallagher & Anderson (1976). Interestingly, already in 1992, Lloyd et al. discussed how the X-ray emission from a nova shell, albeit observed only with a broad-band instrument (*ROSAT*), implies compact clumps in the ejecta as emitting regions.

In our spectral fits, whose parameters are given in Table 2, the appearance of oxygen lines on day 23 depends on the interplay of plasma temperature and emission measure. Increasing the plasma

Table 2. Physical parameters of the fits shown in Figs 2, 4 and 5 (model atmosphere + collisional ionization model BVAPEC in XSPEC). The emission measure is derived from the BVAPEC fit normalization constant assuming a distance of 12 kpc. T_{WD} is the WD effective temperature in the atmospheric model. The flux is in the 0.2–1 keV range, and F_{WD} is the WD atmospheric flux. T_p is the plasma temperature in the BVAPEC model (two regions at temperatures were assumed for a double BVAPEC fit for 2010-02-22). v is the 1σ velocity broadening, F_{tot} is the total flux. The fit with two plasma temperatures also has two different average velocities in the two zones, two emission measures (with the cooler plasma contributing much more) and three values of N(H) (for WD, for the first plasma region at $T_{p,1}$, and for the second plasma region at $T_{p,2}$). The emission lines were also redshifted with redshift z around few times 10^{-3}. A different value of N(H) was used for each of three components in the 02-22 spectrum [while N(H) was unique in the other fits], and we also indicate two velocities for this date, one value for each BVAPEC plasma component. Finally, N/H indicates the nitrogen abundance, the ratio of this element over hydrogen (by mass) over the solar ratio.

Parameter	2010-02-14	2010-02-22	2010-03-05
N(H) (10^{21} cm^{-2})	2	2.7/2.2/2	2.4
T_{WD} (K)	739 000	727 000	1050 000
F_{WD} (erg cm^{-2} s^{-1} $\times$ 10^{-11})	1.79	1.33	1.77
F_{WD} (unabs.) (erg cm^{-2} s^{-1} $\times$ 10^{-10})	3.94	3.9	3.6
$T_{p,1}$ (eV)	93	130	223
$T_{p,2}$ (eV)		182	
Em. measure $\times$ 1.72 $\times$ 10^{57} cm^3	12	32/3	20
N/H	70	20	20
v (1σ, in km s^{-1})	1500	1680/1350	1800
F_{tot} (erg cm^{-2} s^{-1} $\times$ 10^{-11})	2.40	2.46	2.57
F_{tot} (unabs.) (erg cm^{-2} s^{-1} $\times$ 10^{-10})	4.9	4.9	4.22

temperature by only $\simeq$30 per cent, or increasing the emitting volume by a factor of a few (assuming for instance that additional mass is being ejected), the oxygen lines are predicted, but then it becomes difficult to reproduce the other lines, correctly modelled only with a plasma temperature in the 100–120 eV range. The strength of the O VIII Lyα feature is much stronger than all the lines of the O VII He-like triplet, indicating an overlapping component at higher temperature. In conclusion, in order to reproduce both the soft and hard portions of the spectrum, we need at least two components at different temperatures. An additional component at 180 eV reproduces the relative strength of the oxygen features. The component that explains the nitrogen lines, at 120–130 eV, fails instead to reproduce the 'harder' lines. It is thus likely that on day 23 the condensations in which emission lines originated were not at uniform temperature.

5.2 A complicated structure on day 35

We are able to understand the emission line spectra of days 18 and 28 with collisional ionization alone, making the assumptions of clumpiness and adding a second temperature component on day 23, with only 10 per cent of the emission measure of the cooler plasma, and larger oxygen abundance ([O/H] = 1.56 versus only 0.2 in the cooler emitting region). This model thus would also imply either inhomogeneous mixing of the elements in the ejecta or emission of two shells with different abundances. We fitted less accurately the spectrum of day 35, which appears more complex. The emission lines on day 35 remained at least as broad as in the *Chandra* observation of days 18 and 23, while harder flux progressively emerged and lines due to higher ionization stages gradually appeared. However, the spectrum became also more complex and seemed to indicate several different components. The emission lines in Fig. 5 are the same as those of the permanent supersoft X-ray source Cal 87 (see Orio et al. 2004), but the lines were much broader in U Sco.

As shown in the compared fluxed spectra in Fig. 3, on day 35 N VI became much weaker. Fig. 3 also shows that in the N VI He-like triplet and in the O VII triplet on day 35 there is also a definite shift in the relative resonance, forbidden and intercombination line strengths since the February observations. In the February spectra, the resonance line is dominant, but on the day 35, this was still true only for the newly appeared Ne IX triplet, while the resonance lines of the O VII and N VI triplets are weak. For the oxygen triplet, the intercombination line is clearly the strongest.

The line ratios did not become typical of 'simple' photoionization, but we suggest that they are explained with photoionization in the presence of an additional strong UV source, which causes the strong intercombination line and weak forbidden line (see Behar et al. 2004). While the unperturbed value (low density, no UV additional source) of the *f*/*i* ratio is $\simeq$4.4, a much lower ratio like in our case indicates a nearby source of UV flux transferring flux from the forbidden to the intercombination line (Gabriel & Jordan 1969). Since these lines are not eclipsed, we cannot conclude that they were produced close to the WD, so on day 35 at least some of the emission lines were due to photoionization, with a strong, additional UV flux from a nearby region. We hypothesize that this UV flux originated in hot condensations of shocked ejecta.

We also identify iron lines that cannot be explained in the context of either collisional ionization or photoionization, no matter how high the iron abundance. These features are Fe XVII at 16.78 Å (already marginally detected on day 23), Fe XVIII at 14.207 Å and Fe XIX at 14.667 Å. We note that these lines are very typical of quiescent, accreting cataclysmic variables and have been observed also in quiescent novae (Mukai et al. 2003; Mukai & Orio 2005). Mason et al. (2012) attribute also some specific emission features in the optical spectra of U Sco on the very same day to additional emission from the accretion disc. We hypothesize that also these

iron lines, never detected before in previous nova outbursts, arise in an accretion flow. It is significant that they were observed in U Sco, which we know to have resumed accretion early during the outburst, and not in other erupting novae.

Finally, we mention two unsolved problems. Going back to the *Chandra* spectrum of day 18 we see at least one unidentified line at 26.2 Å and possibly one or two at 26.7 and 26.9 Å. These lines are measured with low S/N, but since they were marginally detected also in RS Oph (see Ness et al. 2011b, table 5), they are likely to be real. The second puzzle concerns the N VII Lyα line, which merges with the weaker N VI Heγ line. On day 35, this appears to be a broader and more structured complex than all others. It is certainly much broader than all other lines, and we can only speculate that this line may be produced in several different layers of ejecta with different velocity.

6 CONCLUSIONS

We concluded that the absorption features observed with *Chandra* arose in the WD atmosphere, and the velocity dropped close to zero at the base of the WD atmosphere in the following days, so that the absorption lines were hidden almost at the centre of the broad emission features in the spectra taken with the *XMM–Newton* RGS on days 23 and 35. Fig. 7 shows in fact how the apparent red emission wings of the N VII and N VI lines receded towards zero velocity, as their profiles gradually became symmetric (Fig. 8). The profiles of emission lines that do not have corresponding strong WD atmospheric absorption features, in stark contrast with the N VI and VII features shown in Fig. 7, were almost symmetric around the rest wavelength from the beginning.

From these observations, we inferred that the nova wind almost completely ceased between days 18 and 23 after the optical maximum. No other RN or classical nova has been known to have such a short mass-loss period, and also the short optical light-curve decay time and the large velocity measured in optical spectra were extreme for U Sco.

We agree with previous interpretations of the X-tray eclipse observed on days 23 and 35. It must be due to a Thomson scattering corona, and we propose that the eclipses, although not occurring during the exposures, already existed on day 18. Because of the inclination angle of U Scorpii, we did not observe the hot WD directly, but we mostly measured the flux from Thomson scattered radiation, which conserves the WD spectral shape and features, but gives a lower limit on the true WD luminosity.

Atmospheric models indicate that the WD was already extremely hot on day 18 and reached almost 1000 000 K on day 35. This high temperature is expected only for WD with mass close to the Chandrasekhar limit, above 1.3 $M_{\odot}$.

We find that collisional ionization explains the X-ray emission lines observed in the 2010 February spectra of days 18 and 23. This conclusion is unexpected for a nova without copious circumstellar material around the system. In RS Oph, the red giant wind has left so much dense material that violent shocks can be expected (O'Brien & Lloyd 1994; Nelson et al. 2008). In U Sco the emission line spectrum is in the very soft energy range, unlike in RS Oph. In any case, the only conclusions we can draw from the X-ray spectral diagnostics are that mass-loss was *not* a smooth process. Faster material probably collided with slower one emitted just a few days earlier, and the ejecta had condensations or clumps of dense material that emitted the accretion lines. This may indicate also non-isotropic outflows, or even small clumps like in the old shell of T Pyxidis (Schaefer et al. 2010).

The line ratios and the absence of radiative recombination continua rule out photoionization at least in February, but it seems clear that mass-loss in this nova was not a smooth, continuous phenomenon. A description of the nova in terms of a steady radiation wind (see e.g. Hachisu & Kato 2010, and references therein) probably describes only slow novae accurately, while in cases of fast and frequent outbursts the physics of the mass outflow seems to become quite complicated.

On day 35, after mass-loss from the system had ended, the emission line spectrum became more complex. We identified different components, including collisional ionization, photoionization in presence of an additional UV source, and emission lines of iron, associated with the resumed accretion and probably not with the ejecta. We have not been able to fit all the spectral characteristics of the three spectra accurately, but we propose a sort of 'zero-order model', making a first step in the direction of physical understanding. We examined and analysed in this paper the complexity and non-homogeneity of a nova shell and its evolution.

X-ray grating observations of novae are precious not only because they allow us to probe the WD peak temperature, temperature evolution and effective gravity, but also because of what we can learn on the mass outflow itself. It seems that there is still much work ahead of us – both modelling and observing new outbursts – in order to describe the nova physics accurately. Novae are such interesting laboratories of extreme physics, that we think they are worth the effort.

REFERENCES

Anupama G. C., Dewangan G. C., 2000, AJ, 119, 1359
Balman S., Krautter J., Ögelman H., 1998, ApJ, 499, 345
Barlow M. J. et al., 1981, MNRAS, 195, 61
Behar E., Leutenegger M., Doron R., Güdel M., Feldman U., Audard M., Kahn S. M., 2004, ApJ, 612, L65
Brinkman A. C. et al., 2000, ApJ, 530, L111
Cash W., 1979, ApJ, 228, 939
Chen H., Beiersdorfer P., Heeter L. A., Liedahl D. A., Naranjo-Rivera K. L., Träbert E., Gu M. F., Lepson J. K., 2004, ApJ, 611, 298
Drake J. J., 2003, ApJ, 584, 548
Dürbeck H. W., Dümmler R., Seitter W. C., Leibowitz E. M., Shara M. M., 2003, The Messenger, 71, 19
Gabriel A. H., Jordan C., 1969, MNRAS, 145, 241
Gallagher J. S., Anderson C. M., 1976, ApJ, 203, 625
Hachisu I., Kato M., 2010, ApJ, 709, 680
Kahabka P., Hartmann H. W., Parmar A. N., Neguerela I., 1999, A&A, 347, L43
Kinkhabwala A. et al., 2002, ApJ, 575, 732
Lloyd H. M., O'Brien T. J., Bode M. F., Predehl P., Schmitt J. H. M. M., Truemper J., Watson M. G., Pounds K. A., 1992, Nat, 350, 222
Mason E., Ederoclite A., Williams R. E., Della Valle M., Setiawan J., 2012, A&A, 544, 149
Maxwell M. P. et al., 2012, MNRAS, 419, 1465
Mukai K., Kinkhabwala A., Peterson J. R., Kahn S. M., Paerels F., 2003, ApJ, 582, 184
Mukai K., Orio M., 2005, ApJ, 622, 602
Neff J. S., Smith V. V., Katelsen D. A., 1978, ApJS, 38, 98
Nelson T., Orio M., Cassinelli J. P., Still M., Leibowitz E., Mucciarelli P., 2008, ApJ, 673, 1067
Ness J.-U. et al., 2001, A&A, 367, 282
Ness J.-U., Brickhouse N. S., Drake J. J., Huenemoerder D. P., 2003, ApJ, 598, 1289
Ness J.-U. et al., 2011a, The X-ray Universe 2011, Presentations of a Conference held in Berlin, 27–30 June 2011
Ness J.-U. et al., 2011b, ApJ, 733, 70
Ness J.-U. et al., 2012, ApJ, 745, 43

O'Brien T. J., Lloyd H. M., 1994, MNRAS, 271, 155
Orio M., Nelson T., Gallagher J., 2011, HEAD Meeting, 12.11.06
Orio M., 2012, in Di Stefano R., Moe M., Orio M., eds, Binary Paths to Type Ia Supernovae Explosions. Cambridge Univ. Press, Cambridge, in press
Orio M., Hartmann W., Still M., Greiner J., 2003, ApJ, 594, 435
Orio M., Ebisawa K., Heise J., Hartmann J., 2004, Revista Mexicana de Astronomia y Astrofisica, 610, 194
Pinto C. et al., 2012, A&A, 543, 134
Rauch T., Orio M., Gonzales-Riestra R., Nelson T., Still M., Werner K., Wilms J., 2010, ApJ, 717, 363
Schaefer B. E., 1990, ApJ, 355, L39
Schaefer B. E., 2011, ApJ, 742, 112
Schaefer B. E., Ringwald F. A., 1995, ApJ, 447, L45
Schaefer B. et al., 2010, AJ, 140, 925
Schaefer B. et al., 2011, ApJ, 472, 113
Starrfield S., Sparks W. M., Shaviv G., 1988, ApJ, 325, L35
Thoroughgood T. D. et al., 2001, MNRAS, 327, 1323
Tofflemire B., Orio M., 2012, preprint
Yamanaka M. et al., 2010, PASJ, 62, L37
Yaron O., Prialnik D., Shara M. M., Kovetz A., 2005, ApJ, 623, 398

This paper has been typeset from a TEX/LATEX file prepared by the author.